Anatomically accurate finite element model of a human head for crash applications

Alberto Tacchi, Ivan Colamartino[1], Gabriele Canzi[2], Giorgio Novelli[3], Marco Anghileri[4]

[1] Department of Mechanical Engineering, Politecnico di Milano, Italy
[2] Maxillofacial Surgery Unit, Emergency Department, ASST Grande Ospedale Metropolitano Niguarda
[3] O.U. Maxillofacial Surgery, Department of Medicine and Surgery, School of Medicine,Fondazione IRCCS San Gerardo dei Tintori Hospital, University of Milano-Bicocca
[4] Department of Aerospace Science and Technology, Politecnico di Milano, Italy

1 Introduction

Every year road traffic accidents are responsible of approximately 1.3 million deaths in the world, resulting in one of the main causes of mortality. According to the World Health Organization (WHO), by the 2020s road traffic accidents will be the leading cause of premature death. Moreover, between 20 and 50 million people involved in incidents suffer non-fatal injuries, most of them leading to disabilities [1]. These injuries considerably affect individuals, their families, and nations from both social and economic points of view. Over the last 60 years, experimental activities focused on the impact behavior of the human body were carried out with crash dummies and human cadavers, expanding the available injury database, exposing the most common injury scenarios and allowing the development of effective predictive criteria. The most frequently injured body regions resulted to be head and lower limbs; however severe to fatal injuries (Abbreviate Injury Scale values AIS 3+), are more commonly related to head impacts, as shown in Figure 1 [2].
Different locations of impact (frontal, occipital and temporo-parietal) were investigated with Post-Mortem Human Subjects (PMHS) ([3], [4], [5], [6], [7]), showing that injuries strongly depend on the patient's head morphology. In fact, the range of 50% limit of skull fracture is wide (1800–12500 N), and prediction of minor injuries with simple global criteria based on the cited investigations is inevitably difficult, when feasible.
Over the last two decades, the aforementioned experimental studies allowed the construction of finite element numerical models, and as ethical issues limit nowadays the conduction of further experimental campaigns, today numerical simulations of head impacts are of notable importance in many applications: accident reconstruction in forensic engineering, vehicles' design and development of protection devices, studies on injury prediction for evaluation of suited surgical treatments. Several numerical models of the human body and head have been developed, achieving high levels of detail and accuracy: THUMS [8], VIVA [9] are few notable names. Such models have generally been – and still are today – targeted to the evaluation of global injury criteria for the correlation with dummies used in crash tests, from which simple output information are inevitably extracted, and to numerical robustness and efficiency for their suitability in use with large models. Consequently, biofidelic geometric and material modelling of the human body in crash applications has often been overlooked.

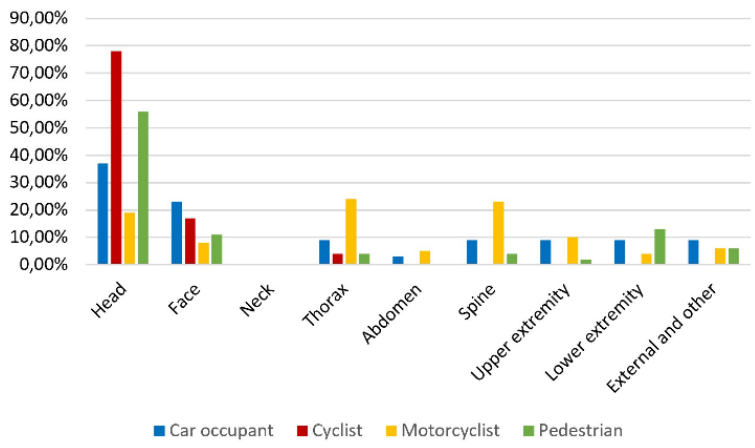

Fig.1: Statistics of AIS 3+ injuries per body regions.

However, experiments on PMHS showed that when head traumas are evaluated accurate geometry reproduction has a key role, and obtaining information about the fracture pattern is fundamental to grasp the real severity of the trauma. As global skull failure criteria cannot provide reliable information about the fracture pattern ([10], [11]), in the last few years studies increased the anatomical representation of the skull geometry using CT scans, considering the bone constituted of both its compact and cancellous parts ([12], [13]).
Accordingly, the present work intended to provide a complete FEHM targeted to reliable reproduction and prediction of head impact events, characterized by an accurate anatomical geometry based on medical CT images, modelled with constitutive laws that consider the non-linear material behavior and failure mechanisms. The FEHM presented in [12] provided the main reference, especially in terms of geometry and material models. The skull was then modelled with a stress triaxiality dependency, a novel concept in the numerical modelling of impact biomechanics, showing great potential in fracture pattern prediction. The model was subsequently validated against solid experimental literature. Last, an investigation of a real-world road accident was conducted with the new FEHM to preliminary assess the skull damages and brain injuries sustained upon collision.

2 Materials and methods

Primary attention was devoted on developing an accurate anatomical geometry of the skull starting from medical high-quality CT scans (498 images, 512 x 512 scanning matrix, slice thickness = 1 mm, slice increment = 0.5 mm). The patient is an adult male without pathologies whose physical characteristics are compatible with the 50th-percentile adult male definition (ISO 15830-1 [14]). Differently from most of the existing FEHMs, skull features such as separation of cortical bone, diploë and sutures, and paranasal sinuses are preserved in this model, reaching a superior level of detail. The use of Materialise Mimics (Materialise NV) allowed to obtain the desired geometry through both automatic and manual segmentation processes. On the contrary, since brain injuries have a marginal role in this study, a simplified geometry of the intracranial content has been considered. Due to the non-availability of Magnetic Resonance Imaging (MRI) images of the patient, the brain was built using an internal offset of the cranial vault and base of the skull. Similarly, the scalp is a constant thickness offset layer of the external surface of the skull.
The achievement of an anatomically faithful configuration was possible through the solid modelling of linear tetrahedron elements, suitable for developing convoluted and complex shapes. The resulting mesh has an average size of 2 mm, leading to a complete FEHM with over 2 million solid elements. Table 1 reports detailed mesh information.

Component	Type of elements	Number of elements	Number of nodes	Min / Average size of elements (mm)
Skull	Linear tetrahedron	794784	170138	1.3 / 1.9
CSF	Linear tetrahedron	290684	71571	1.5 / 2.1
Brain	Linear tetrahedron	490413	93950	2.0 / 2.8
Scalp	Linear tetrahedron	478754	98984	1.8 / 2.2

Table 1: FEHM's mesh information".

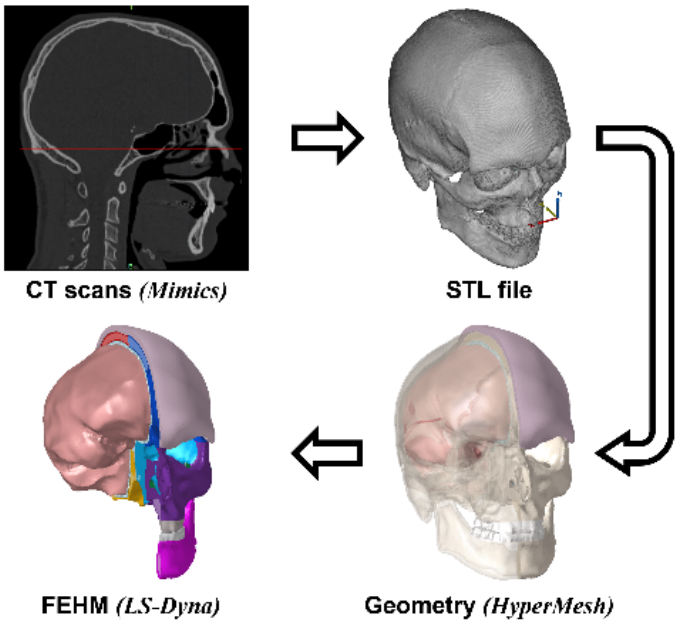

Fig.2: Medical images, geometry and FEHM.

If the mandibular contribution is surely of great importance in head injuries reconstruction, a proper reproduction necessarily comes with a suited modelling of the joint and possibly muscle activation, beyond the scope of the present work. Consequently, although the mandible was meshed and included in the model, it was not considered for the rest of the work and proper mandible coupling left to future developments. The finalized FE model of the skull, counting 2054635 elements and 434643 nodes, is shown in Figure 3.

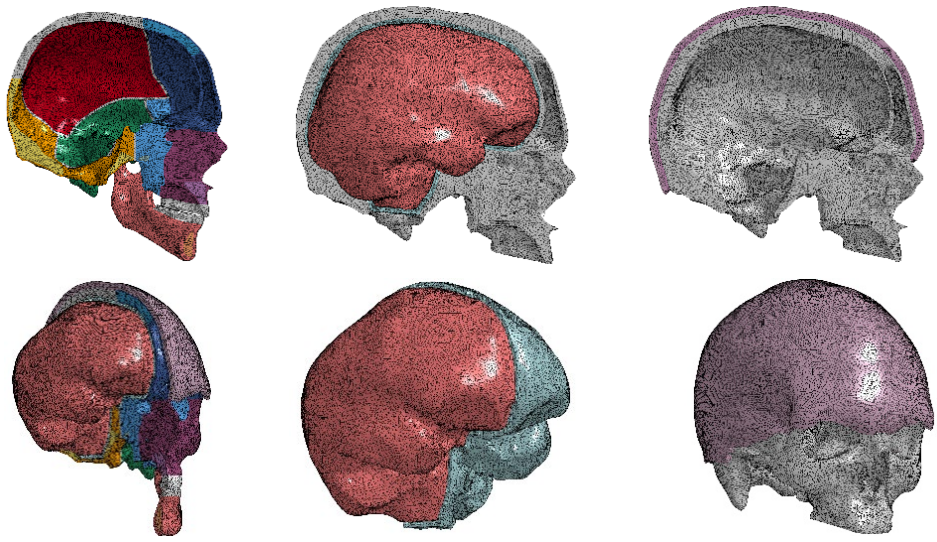

Fig.3: Lateral and isometric views of the FEHM.

2.1 Material models

The model was developed for the explicit finite element software Ansys LS-DYNA, hence some of the following information are given in accordance with the software.
The fine mesh of the model was suitable to study the fracture mechanism of hard tissues, thus advanced material modelling techniques were exploited accordingly. It was assumed that failure of compact bones,

much stiffer and stronger than trabecular bones, always results in skull fractures: as such, the focus was mainly devoted to model the material of compact bones whereas minor adjustments were performed on sutures and diploë. Since material behave differently depending on the loading condition (compression or tension) it was decided to exploit the material *MAT124_PLASTICITY_COMPRESSION_TENSION where independent yield stresses as a function of plastic strain curves can be defined for compression and tension. The properties of the bones were extracted from [15], where the mechanical behavior of human femoral cortical bone was investigated both in compression and tension. However, since femur and skull have different material properties since they are a long and an irregular bone respectively, the femoral compressive behavior was scaled according to known parameters of the skull, the ultimate compressive stress. Regarding diploë and sutures, they were assumed to be perfectly isotropic and modelled with a piecewise linear plastic model, through the material card *MAT024_PIECEWISE_LINEAR_PLASTICITY. The properties for both diploë and sutures employed in this work were derived from THUMS v6 (AM50 occupant) and [12]. Figure 4 shows piecewise linear curves used for describing the behavior of skull bones.
The non-linear behavior of soft tissues (brain and scalp) was implemented with the card *MAT061_KELVIN-MAXWELL_VISCOELASTIC, a viscoelastic model whose shear modulus is defined in (equation 1):

$$G(t) = G_\infty + (G_0 - G_\infty)e^{-\beta t} \qquad (1)$$

where the viscoelastic effect in shear is defined with a deviatoric stress rate dependent on the shear relaxation modulus.
Scalp-skull and skull-brain interfaces were modelled as a sliding interface, allowing the relative motion and contact between components for accurate reproduction of the head response. The cerebrospinal fluid surrounding the brain was defined as a solid layer characterized by an elastic fluid material.

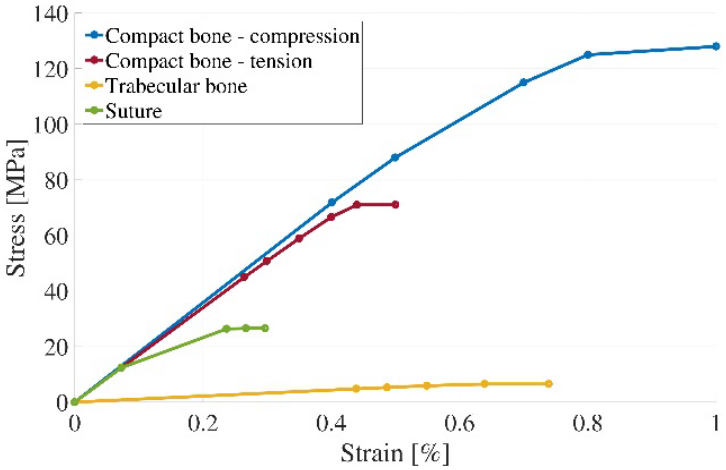

Fig.4: Numerical piecewise linear stress strain curves for tables, diploë and sutures.

2.2 Fracture model

Upon a collision, the bone tends to initiate the fracture mechanism due to the out-of-plane bending of the region surrounding the impact site; hence, the tensile strain failure threshold is commonly the most critical value. However, the use of a single, and the lowest, threshold could lead to a premature and/or incorrect crack initiation and therefore the concept of triaxiality was exploited to implement the whole range of state-of-stresses into the failure model. As mentioned above, since tables are stiffer than diploë, when the former break the diploë is assumed to be ruptured as well: consequently, the failure model was implemented for compact bones only.
Triaxiality defines the fracture locus in terms of failure strain as function of a non-dimensional parameter named stress triaxiality (equation 2):

$$\epsilon_f = f(\sigma^*) \qquad (2)$$

The stress triaxiality parameter, σ^*, describes the current state of stress acting on three-dimensional elements, and is defined as the ratio between the hydrostatic stress σ_h and an equivalent stress usually taken as the Von Mises stress σ_{vm} (equation 3):
The strain failure locus shown in Figure 5 was derived from a triaxiality curve experimentally extracted for a steel alloy and scaled down on the known failure threshold in pure tension ($\sigma^* = 0.33$). Finalized compact bone triaxiality curve is showed in figure 5.

$$\sigma^* = \frac{\sigma_h}{\sigma_{vm}} \qquad (3)$$

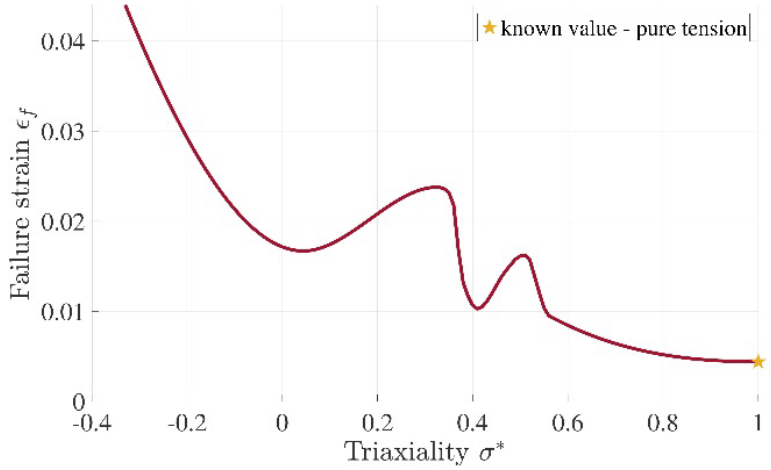

Fig.5: Numerical piecewise linear stress strain curves for tables, diploë and sutures.

2.3 Geometric and mass information

Reference values of the head model were useful to conduct a cranial anthropometry comparison between the numerical model and the tested specimens before performing the simulations.

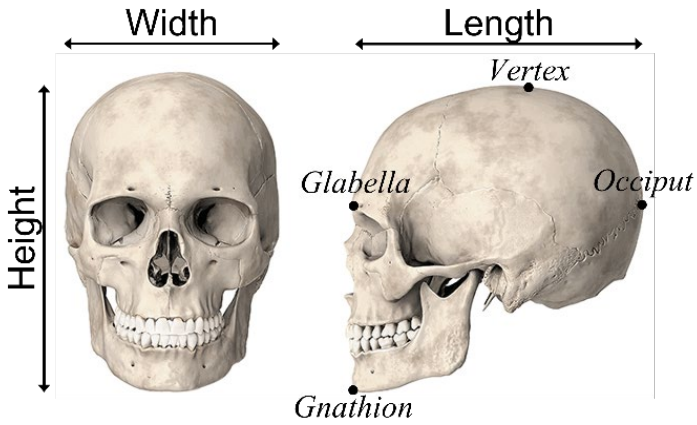

Fig.6: Scheme of physical data measurements.

A [cm]	B [cm]	C [cm]	D [cm]	E [cm]	F [cm]	G [kg]
14.6	19.4	22.4	16.0	55.3	0.6	3.2

Table 1: Mass and geometric information: A) skull width (maximum above ears), B) skull length (nasion to occiput), C) skull height (gnathion to vertex, D) skull height (cranial base to vertex), E) skull circumference, F) scalp thickness at the impact sit, G) head mass.

3 Results and discussion

A four-step literature-based validation procedure, schematically showed in Figure 7, was followed. Each step was preceded by cranial anthropometry comparison with the head subject to prevent non-acceptable dimensional deviations.

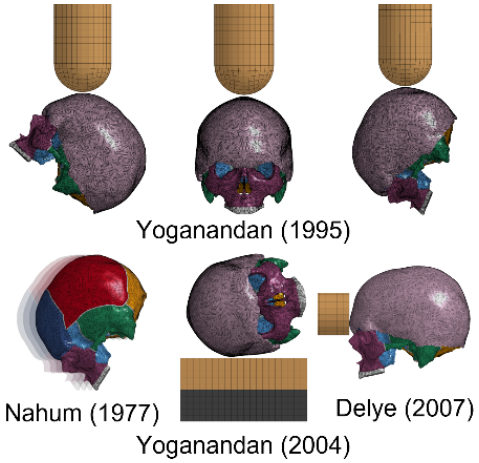

Fig.7: Settings of numerical simulations

3.1 Intracranial pressure

The first step was based on a series of experimental frontal impacts reported in [3] measuring the intracranial pressures at four different sites: frontal, parietal, occipital and posterior fossa. The experiment was reproduced prescribing the known velocity to nodes belonging to the skull and allowing free movement of the brain, consequently subjected to both coup and contrecoup phenomena in the anterior and posterior regions respectively.

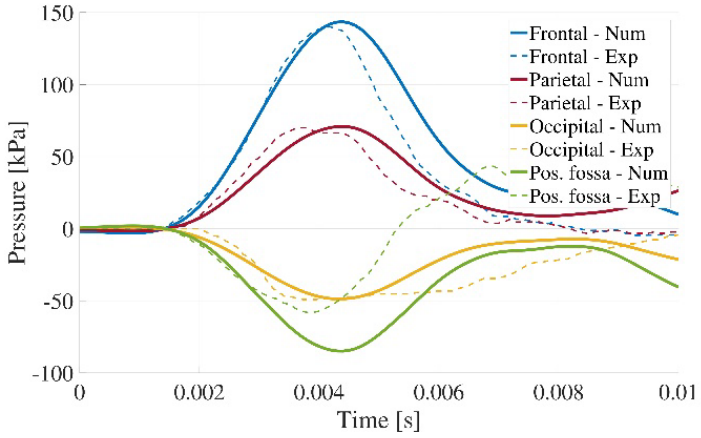

Fig.8: Brain pressures

Minor numerical inaccuracies were recorded: despite the use of one-point constant stress tetrahedrons with nodal pressure averaging formulation, solid formulation 13 in LS-DYNA, a volumetric locking phenomenon was observed at the posterior fossa with largest discrepancies reported for the pressure at the base of the head, as visible in Figure 9. Such phenomenon, which can be detected through its typical “checkerboard” pattern was however confined to a small portion in correspondence of the foramen magnum.

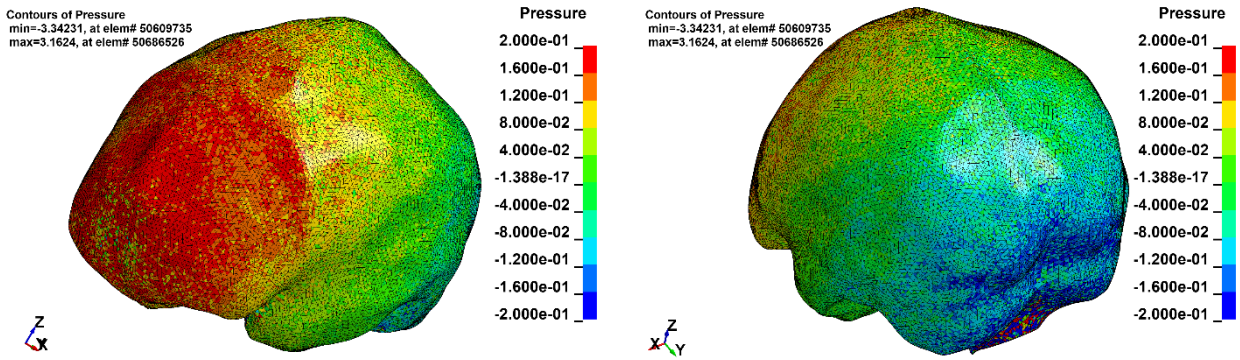

Fig.9: Coup and countercoup phenomena

Considering the results presented in figure 8 and the negligible numerical issues, this first step was considered a first validation in terms of the relative motion between the skull and the scalp as well as the materials of intracranial contents.

3.2 Blunt impacts

Yoganandan [5] performed a series of blunt impacts of a rigid hemispherical anvil with stationary cadavers' heads useful to validate both the material elastoplastic curves and the scalp model. Collisions occurred in correspondence of frontal, vertex and rear portion of the skull while the head was fully constrained at the base. Tested velocities ranged from 7.1 to 8 m/s, with an average input energy of approximately 68 J.

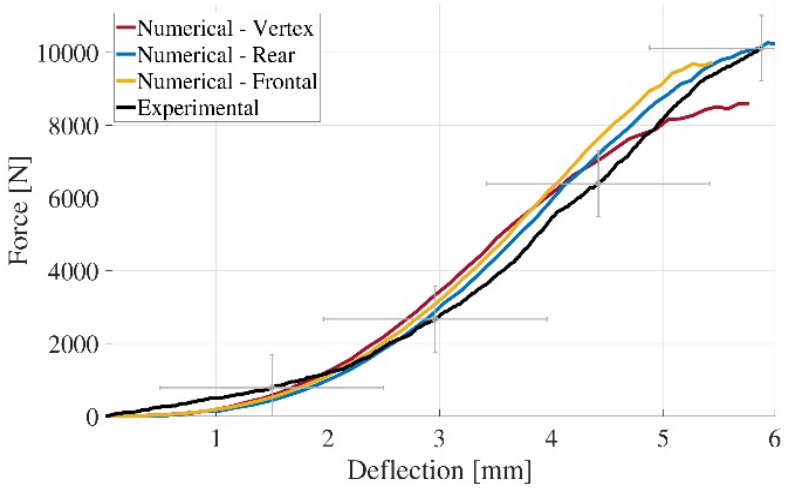

Fig.10: Comparison of force-deflection curves

As shown in Figure 10, the resulting force-deflection curve matches well the experimental results. An initial non-linear region highlights the non-linear behavior of the scalp, a subsequent quasi-linear portion reflects the response of the skull while deforming until fracture occurs with maximum deflection of 6 mm. Yoganandan [5] also reported the presence of circular fracture at vertex and rear; similarly, the model reported circular failure patterns, validating the material model with good correlation.

3.3 Lateral free-fall impacts

A series of lateral impacts with the free-fall technique were conducted by Yoganandan [6]. A system of three accelerometers was attached to the skull, at anterior, contra-lateral and posterior locations, to measure linear acceleration histories. Free-fall tests were performed at low, intermediate and high velocities: 3.5 m/s, 4.9 m/s and 6.0 m/s respectively. The head impacted against a rigid padding layer instrumented with a load cell.
The numerical setup has faithfully reproduced the experiments, leading to a globally good correspondence of results in terms of linear accelerations and input force. As expected, accelerations differ from one site to another, verifying that the skull does not behave like a rigid structure. Highest magnitude was obtained for the occipital bone, which is, according to medical studies, the strongest one, followed by side and front.

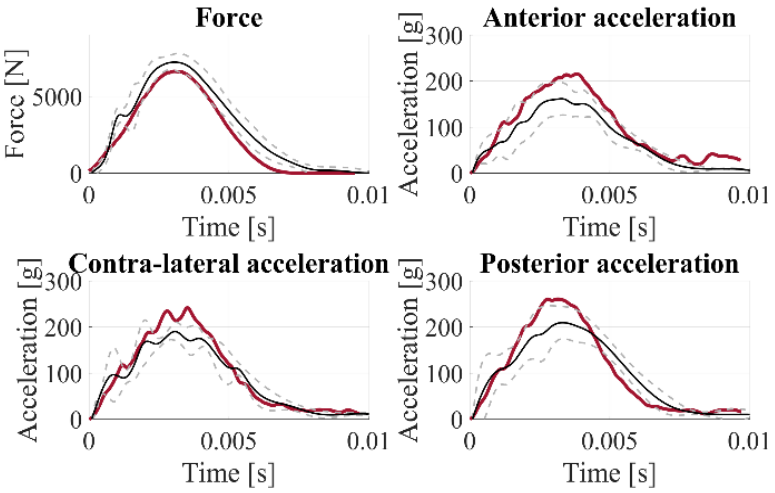

Fig.11: Force (left top), and acceleration (anterior — right top, posterior — right bottom, contra-lateral — left bottom) responses at 4.9 m/s impact velocity. Black solid and dashed lines refer to experimental corridors expressed as mean ± their standard deviation. Red solid lines are the numerical results.

All numerical simulation and most of experimental test obtained severe HIC (HIC>1255 and AIS 3+) without occurrence of fractures.

3.4 Frontal impacts

The fourth step was performed to validate the bone fracture model. Delye [7] performed frontal impacts at different levels of input energy, employing a double-pendulum system constraining the head on the upside-down position, leaving free movement within the mid-sagittal plane. The initial potential energy of the impactor was variated between the experiments by changing the mass and the initial position of the pendulum.
Two experimental cases have been considered: the first was a single test performed at 214.33 J with the mass travelling at 3.39 m/s, the second was a series of tests where the mass ranged from 37.3 to 48.3 kg, whereas the input energy ranged from 502.36 to 655.53 J.

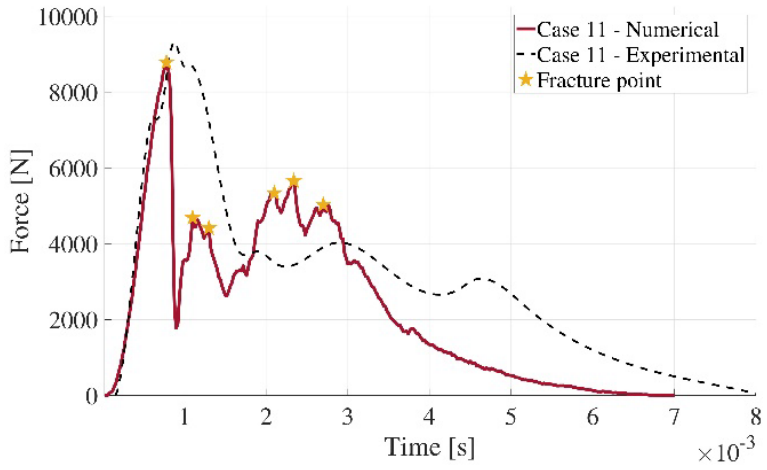

Fig.12: Numerical force response - Case 11

A comparison between force-time histories is shown in Figure 12. The numerical curve well captures the experimental results, showing not only an optimal correlation of the first peak force, but also good correlation of the fracture initiation instant. Moreover, the visual correspondence with the fracture propagation has allowed to identify subsequent crack openings and depressed fracture typical of collisions with small contact areas.
Figure 13 shows the fracture propagation at subsequent instants.

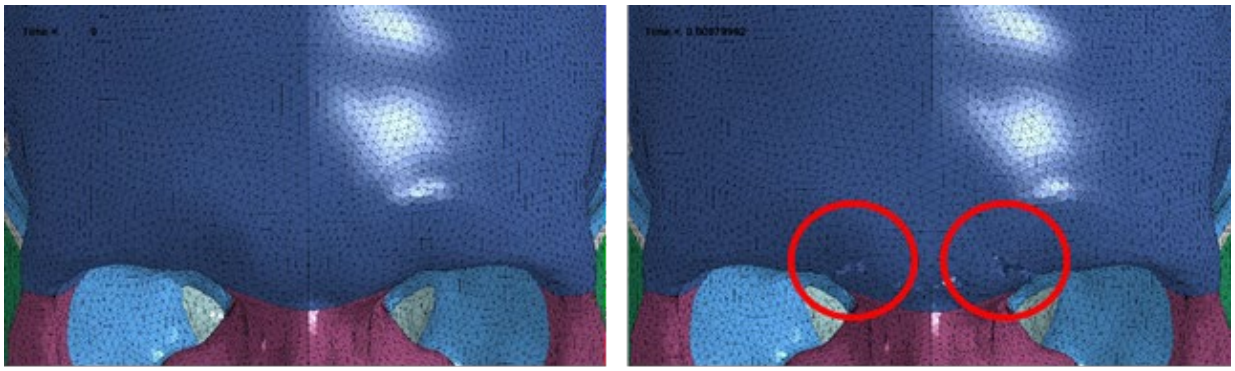

(a) $Time = 0.0\ ms.$ (b) $Time = 0.8\ ms.$

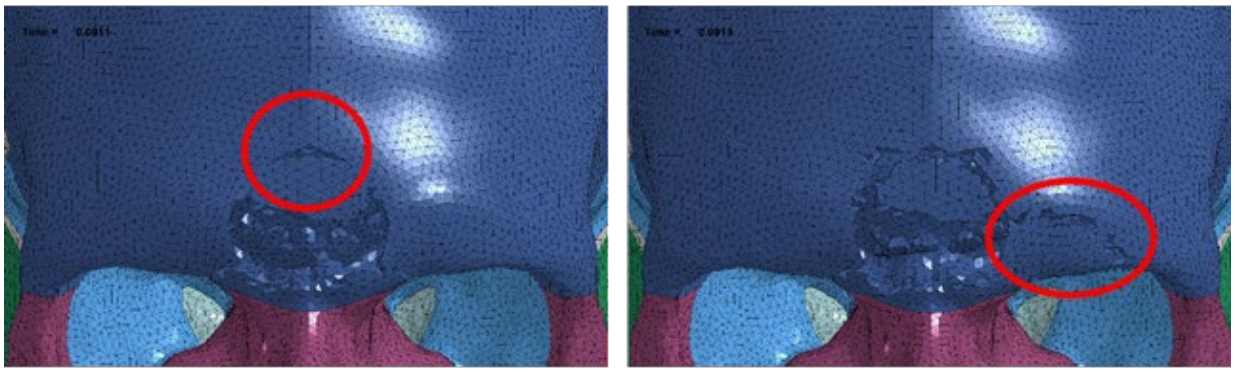

(c) $Time = 1.1\ ms.$ (d) $Time = 1.3\ ms.$

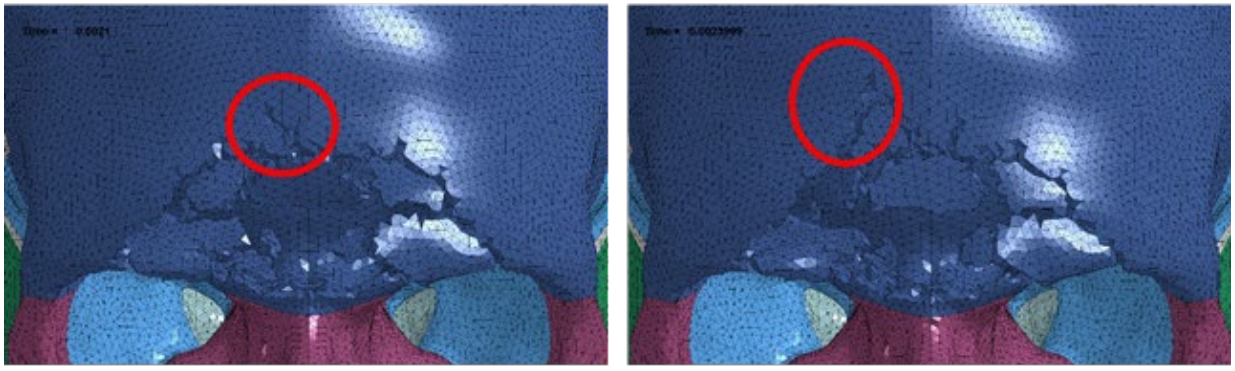

(e) $Time = 2.1\ ms.$ (f) $Time = 2.3\ ms.$

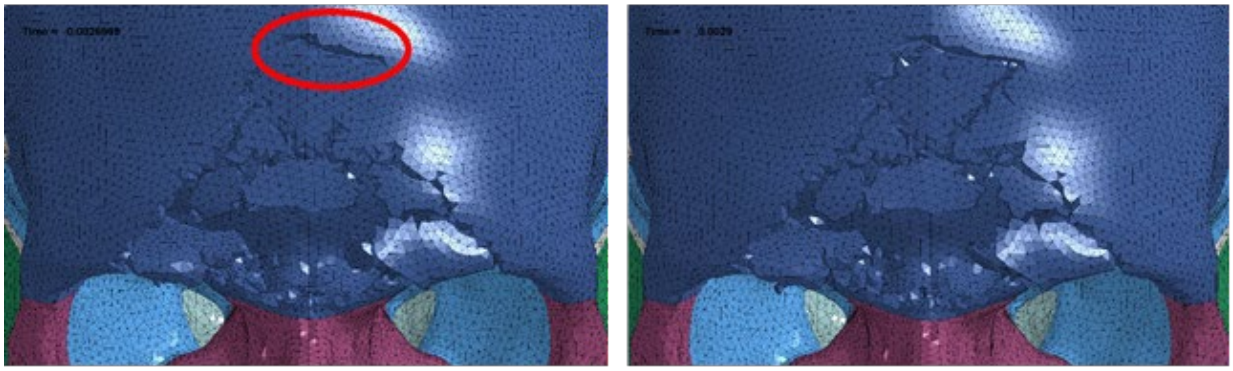

(g) $Time = 2.8\ ms.$ (h) $Time = 3.0\ ms.$

Fig.13: Numerical force response - Case 11

3.5 Computational costs

To run the simulations, the new FEHM required computational time was at least twice more than the THUMS because of the high number of elements. THUMS' results are not shown here as not significant, however detailed comparison in terms of computational costs is shown in figure 14.

3.6 FEHM application to a real-world accident

Once the FEHM has been validated with experimental tests, a real-world scenario is presented: in particular, an application of accident reconstruction.

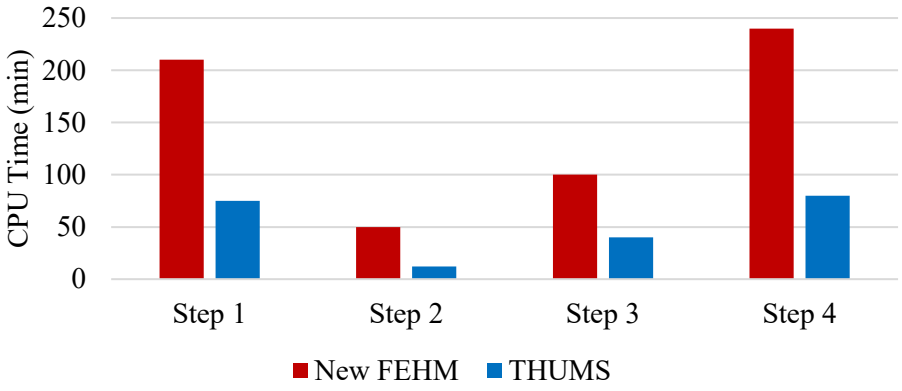

Fig.14: Comparison of validation step simulation CPU time using the new FEHM and THUMS. Simulations were run on an Intel i7-6700, 3.40GHz clock, 6-core workstation.

The model has been employed to investigate the collision occurred between a motorcyclist and a bicycle, in which the former sustained multiple skull fractures after being unsaddled from the motorbike. Little information was available, and only coming from the analysis of the injuries: presence of fracture on the lower part of frontal bone, fracture of the left side of maxilla, linear fracture of the right lateral orbital wall, top-to-bottom and left-to-right directions of the blow, impacted surface of approximately 10 cm. It is on the other hand unknown the nature of the impacting surface, may it be a steel barrier or the ground, as well as unknown are the number of impacts and even approximate values for impact velocities. It is known that the motorcyclist, at the time of the incident, wore an open face helmet; from a safety point of view, such helmet is less effective than a full-face one because it does not provide face protection and can easily fall during collisions. Victims wearing a full-face helmet are consequently at lower risk of sustaining facial injury, compared to those wearing other types of helmets, with an adjusted Odds Ratio (OR) of 0.31 [16]. Last, fundamental information, is the fact that the patient survived the incident, suggesting impact at non-fatal levels of energies/velocities. The few information available are sufficient to setup a series of analysis through the FEHM, targeting the deduction of the most plausible incident dynamics.

The analysis started performing an oblique impact directly against an inclined flat rigid surface prescribing the initial velocity of the head; the considerations on the open-face helmet allowed to immediately neglect the modelling of the helmet. First objective was the identification of the impact speed: three velocities, 18 km/h, 30 km/h and 45 km/h, have been selected to identify the most plausible; to achieve such identification, the visual observation of fracture patterns was the only method available for comparison. The intermediate velocity, 30 km/h, has been identified as best correlated since the size of the fractured area in the frontal bone was similar with respect to medical images. However, maxilla fracture was not reported for any of the three analyzed impact speeds.

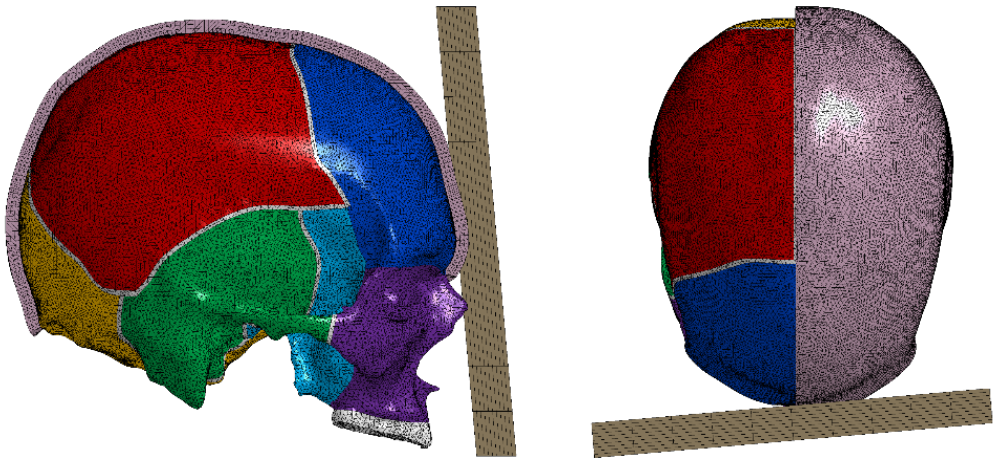

Fig.15: Numerical setup with flat surface

A subsequent analysis was then performed at 30 km/h using a morphing impacting surface to induce failure of the left maxilla: the analysis caused a depressed fracture propagating from the nasal root mostly in horizontal direction, and finally a fracture of the left maxilla was reported (Figure 16).

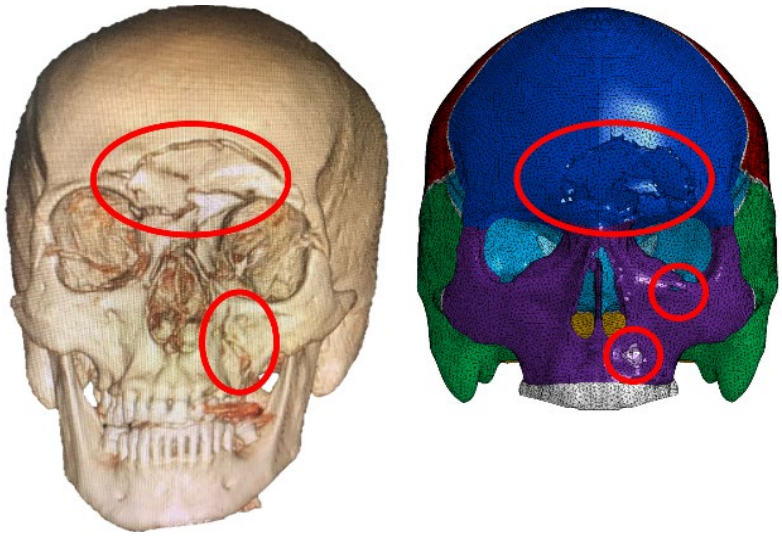

Fig.16: Comparison of fracture patterns, second impact

Consequently, the numerical investigations identified at 30 km/h the most plausible impact speed: however, a single blow to the nasal root does not seem to lead to the fracture of the maxilla, even at higher velocities. This means that the motorcyclist was subjected to multiple subsequent collisions. An HIC value of approximately 1250 suggests the presence of moderate brain injuries, such as mild concussion and minor neurological damages, confirmed by the medical reports. Ultimately, the fact that the subject survived the accident is numerically confirmed, since the non-survivable HIC value of 1860 is not exceeded.
In summary, the numerical investigations through the FEHM allowed to reconstruct the incident dynamics with an accuracy which is difficult to achieve with state-of-the-art techniques, may them be of engineering and medical nature. At the same time, as the HIC values were validated by medical reports, the FEHM showed high versatility, reproducing both fracture patterns and global injury criteria.

4 Conclusions

The main objective of this work was to develop and validate a novel finite element head model for crash applications, with anatomically accurate geometry description and advanced injury reproduction with respect to state-of-the-art human models. The purpose has been achieved with a good correlation between simulation results and experimental results, comparing impact forces, accelerations, absorbed energy, brain pressures and visual fracture patterns.
This study investigated the validity of a strain-based skull fracture criterion with triaxiality implementation. Although failure could be considered more critical in tension due to lower strain failure values, the use of a single threshold common in state-of-the-art solutions, could lead to a premature and/or incorrect crack initiation: the implementation of the strain failure dependency on the current state of stress developed at local level allowed to improve the sustained fracture description, with coherent prediction of fracture patterns, especially concerning depressed fractures.
Injury threshold for the head have been reported, in terms of local parameters, at strain threshold of 0.44%, verified to correctly model the fracture of compact bone in tension, whereas the threshold in compression was found to be ten times higher. In terms of global parameters, the model has confirmed well-known literature values: frontal bones of the present head model showed rupture once the applied force exceeds 6-9 kN, with energy absorption capability of 20-24 J before failing.
In terms of limitations, the model lacks an advanced reproduction of the brain: if global parameters are reproduced with good reliability, local brain injury criteria cannot be used with this model because of the lower precision in predicting stresses and strains within the brain. Minor numerical issues (volumetric locking) were also observed in the lower region of the brain: even if it was verified that these phenomena did not influence the results in the remaining portions of the model, a more accurate modelling of brain with gyri and sulci could improve the results. Nevertheless, the HIC has been confirmed to predict injuries from a global point of view.
Future developments will focus on the mandible coupling as completion of the hard tissue of the head, with attention devoted to model the freely movable joints with activable nerves and muscles. Subsequently, the complete FEHM will be made compatible with THUMS (AM50 V6.1) in order to simulate the whole dynamics of the human body during an accident. Regarding the fracture model, a further experimental validation through the mechanical characterization of the human bone would be essential to derive strain failure thresholds for different stress triaxiality values than the pure tension one. Last, a parametric version of the model is planned to be implemented, targeting the possibility to variate the skull thickness to comply to different patients' head morphologies and consequently investigate the effects of such variations.
In conclusion, the developed FEHM showed suitability and reliability in modelling common crash scenarios of typical road accidents: the model is predictive in terms of fracture pattern description, which is, to the authors' knowledge, a novel result with respect to the state-of-the-art human body models, commonly used for correlation with global criteria and in general with tension-based failure criteria. After validation against literature, a real incident was analyzed and the model proved to be effective in providing useful indication on the dynamics of the incident, based solely on the analysis of the fracture pattern. Even if inevitable drawbacks with respect to standard human body models are found in terms of computational costs' increase, the authors believe that the present numerical model could be useful in terms of predicting and analyzing road accidents involving VRUs (Vulnerable Road Users) such as motorcyclists, cyclists and pedestrians, allowing the appreciation of local injury patterns and consequently lead to better understanding of such patterns, with advantages in terms of design of protection devices, development of standard surgical treatments and forensic procedures, and in general improvement in road safety.

5 References

[1] «Road traffic injuries,» [Online]. Available: https://www.who.int/news-room/fact-sheets/detail/road-traffic-injuries.

[2] S. Piantini, D. Grassi, M. Mangini, M. Pierini, G. Zagli, R. Spina e A. Peris, «Advanced accident research system based on a medical and engineering data in the metropolitan area of Florence,» *BMC Emergency Medicine,,* n. 13, 2013.

[3] A. Nahum, R. Smith e C. C. Ward, « Intracranial pressure dynamics during head impact,» *Society of Automotive Engineers (SAE),* pp. 339-366, 1977.

[4] D. Allsop, T. Perl e C. Y. Warner, «Force/deflection and fracture characteristics of the temporo-parietal region of the human head,» 1991.

[5] N. Yoganandan, F. A. Pintar, A. Sances, P. R. Walsh, C. L. Ewing, D. J. Thomas e R. G. Snyder, « Biomechanics of skull fracture,» *Journal of Neurotrauma,* pp. 659-668, 1995.

[6] N. Yoganandan, F. A. Pintar e J. Zhang, «Force and Acceleration corridors from lateral head impact,» *Traffic Injury Prevention,* pp. 368-373, 2004.

[7] H. Delye, P. Verschueren, B. Depreitere, D. Verpoest, I. Berckmans, J. Vander Sloten, G. Van Der Perre e J. Goffin, «Biomechanics of frontal skull fracture,» *Journal of Neurotrauma,* vol. 24, pp. 1576-1586, 2007.

[8] M. Iwamoto, Y. Kisanuki, I. Watanabe, K. Furusu e K. Miki, «DEVELOPMENT OF A FINITE ELEMENT MODEL OF THE TOTAL HUMAN MODEL FOR SAFETY (THUMS) AND APPLICATION TO INJURY RECONSTRUCTION,» in *Proceedings of the International Research Council on the Biomechanics of Injury Conference, 30*, 2002.

[9] J. John, C. Klug, M. Kranjec, E. Svenning e J. Iraeus, «Hello, world! VIVA+: A human body model lineup to evaluate sex-differences in crash protection,» *Frontiers in Bioengineering and Biotechnology,* vol. 10, 2022.

[10] L. Zhang, K. H. Yang, R. Dwarampudi, K. Omori, T. Li, K. Chang, W. N. Hardy, T. B. Khalil e A. I. King, «Recent advances in brain injury research: a new human head model development and validation,» *Society of Automotive Engineers (SAE),* pp. 369-394, 2001.

[11] S. Kleiven e W. N. Hardy, «Correlation of a FE model of the human head with experiments on localized motion of the brain: consequences for injury prediction,» *Society of Automotive Engineers (SAE),* 2002.

[12] A. Barbosa, F. Fernandes, R. Alves de Sousa, M. Ptak e J. Wilhelm, «Computational modeling of skull bone structures and simulation of skull fractures using the YEAHM head model,» *Biology,* vol. 9, 2020.

[13] D. De Kegel, A. Meynen, N. Famaey, G. van Lenthe, B. Depreitere e J. Vander Stolen, «Skull fracture prediction trhough seubject-specific finite element modelling is higly sensitive to model paramentes,» 2019.

[14] *ISO 15830-1:2022 Road vehicles — Design and performance specifications for the WorldSID 50th percentile male side-impact dummy,* 2022.

[15] E. F. Morgan, F. Fernandes, R. Alves de Sousa e A. I. Hussein, «Bone mechanical properties in healthy and diseased states,» *Annu Rev Biomed Eng,* vol. 20, pp. 119-143, 2018.

[16] D. Wu, M. Dufournet e J. L. Martin, «Does a full-face helmet effectively protect against facial injuries?,» *Injury Epidemiology,* vol. 6, 2019.